IEEE Access
Multidisciplinary | Rapid Review | Open Access Journal

Received November 22, 2018, accepted December 4, 2018, date of publication December 10, 2018, date of current version January 7, 2019.

Digital Object Identifier 10.1109/ACCESS.2018.2885856

Adaptive Covariance Feedback Cubature Kalman Filtering for Continuous-Discrete Bearings-Only Tracking System

RENKE HE[1], **SHUXIN CHEN**[1], **HAO WU**[1], **HAN XU**[1], **KUN CHEN**[2], **AND JING LIU**[1]
[1]Information and Navigation College, Air Force Engineering University, Xi'an 710077, China
[2]Air Force Harbin Flight Academy, Harbin 150000, China

Corresponding author: Hao Wu (wuhaostudy@163.com)

This work was supported by the National Natural Science Foundation of China under Grant 61673392 and Grant 61703420.

ABSTRACT Bearings-only tracking is a continuous-discrete system, whose state of motion is in the continuous-time domain and the measurement is in the discrete-time domain. The unpredicted approximation errors are inevitable due to integration, discretization, and linearization of continuous model in many filtering methods. The adaptive covariance feedback framework is proposed for solving this kind of problem, in which the posterior covariance sequence is proved theoretically to be useful for prior covariance updating. In this framework, the covariance feedback framework is integrated with the continuous-discrete cubature Kalman filtering, and Chebyshev distance is applied to judge the proper condition for the start-up of the feedback channel. The numerical results illustrate the proposed method's superior performance in accuracy and computational efficiency.

INDEX TERMS Cubature Kalman filtering, bearings-only tracking, nonlinear filtering, continuous-discrete systems.

I. INTRODUCTION

Bearings-only tracking (BOT) [1] is applied widely for navigation [2], passive tracking [3], etc., in which only the bearings information is used for target location or tracking. In general, the forms of the measurement function and the state function are discrete in the conventional filtering methods. The advantages of the discretized form are obvious that it is easy for mathematical deduction and computation. Actually, the state model in BOT can be embodied completely within continuous-time form, which is more accurate than the traditional discretized forms [4]. In this work, BOT is described as a continuous-discrete (CD) system.

Compared with the conventional discrete-time domain filtering methods, the form of state prediction is quite different. The state is described as the stochastic differential equation (SDE). The form of SDE makes the mathematical deduction more complex in CD filtering methods. Itô calculus and Stratonovich calculus [5] are two main means to solve the special SDEs problem in many researches. In [6], Itô-type stochastic differential system model and ensemble Kalman filter are used to improve the accuracy of state estimation for a nonlinear CD model.

In general, the numerical approximate methods are applied for the solving differential equations, such as Taylor approximation and Runge-Kytta approximation. In [7], Itô-Taylor expansion of order 1.5 is used to approximate the state model, and cubature Kalman filtering (CKF) for CD systems is proposed. In [8], the order 0.5 Euler-Maruyama filtering method is introduced, and the Euler scheme of SDE is applied in the method to achieve the 0.5 rate of convergence. In [9], Runge-Kytta approximation and the unscented Kalman filtering (UKF) are used for a nonlinear continuous-time stochastic system. The higher order Runge-Kytta approximation methods are reviewed in [4]. In [10], the deterministic Runge-Kytta algorithms and a moment matching technique are used to predict the target state and covariance matrix. In [11], the adaptive Markov chain Monte Carlo (AMCMC) based numerical integration method is proposed for parameter estimation in nonlinear SDEs, and the performance is better than the Taylor series and particle MCMC approximations.

No matter what kind of approximation method is used, the focus of most researches is on the accuracy, robustness and computational efficiency, etc. In [12], the feedback

2169-3536 © 2018 IEEE. Translations and content mining are permitted for academic research only.
Personal use is also permitted, but republication/redistribution requires IEEE permission.
See http://www.ieee.org/publications_standards/publications/rights/index.html for more information.

particle filter algorithm is introduced for the CD nonlinear filtering problem. An error-based feedback control structure is proposed to improve the accuracy of the algorithm. In [13], a variable-size unscented Kalman filter is proposed to deal with CD stochastic models in radar tracking, in which the global error control ensures the better accuracy and efficiency compared with the accurate continuous-discrete extended Kalman filter (ACD-EKF) and the accurate continuous-discrete extended-unscented Kalman filter (ACD-EUKF). Similarly, in [14], the variable-step-size Gauss- and Lobatto-type Nested Implicit Runge-Kutta (NIRK) formulas of orders 4 and 6 are presented, and the automatic local and global error regulation mechanisms are implemented in the method. In [15], the accurate continuous-discrete method and CKF are combined in the proposed method, in which the time updating is implemented in the accurate continuous-discrete method while the measurement updating is implemented in CKF based on the third-degree spherical-radial cubature rule. Ogihara and Tanaka [16] deduce the asymptotic error distribution of the Euler method for nonlinear CD filtering problem, and the stable convergence is proved. However, discretization and linearization, the unknown approximation errors cannot be avoided by the method mentioned above. In [17], a feedback CD-EKF framework of the covariance adaption is proposed; the posterior covariance information is used for the prior covariance updating. However, it is suboptimal to use EKF framework for nonlinear filtering problem.

To alleviate effects of unpredictable errors, the adaptive stochastic feedback method is proposed. The posterior covariance sequence is proved theoretically to be useful for prior covariance updating. Thus, the stochastic feedback based covariance online adaption channel is established. To cope with the nonlinear filtering method, the channel is integrated with the framework of CD-CKF, in which the Chebyshev distance is used as a threshold to determine whether to trigger the online adaption mechanism or not.

The paper is structured as follows: section II presents the BOT model. Section III briefly introduces the general types of continuous-discrete filters. Section IV deduces the covariance updating method and presents the adaptive stochastic feedback framework of CD-CKF (ASFCD-CKF). Simulations results are shown in section V, and section VI concludes the main work.

II. THE MODEL OF BOT

The model of BOT contains the state function and measurement function, where the state function is in continuous time-domain and the measurement function is written as the discrete form. Suppose that the state is in 2-dimensional Cartesian coordinate. The model with CD form can be rewritten as

$$d\boldsymbol{x}(t) = \boldsymbol{f}(\boldsymbol{x}(t), t)dt + \sqrt{\boldsymbol{Q}}d\boldsymbol{w}(t) \tag{1}$$

$$z_k = h(\boldsymbol{x}_k, k) + e_k, \quad k = 1, 2, \cdots \tag{2}$$

$$h(\boldsymbol{x}_k, k) = \arctan \frac{x_k}{y_k} \tag{3}$$

where the state $\boldsymbol{x}(t) = [x(t), y(t), \dot{x}(t), \dot{y}(t)]^T$ is the state of the target. The position and velocity are $\boldsymbol{x}^p(t) = [x(t), y(t)]$ and $\boldsymbol{x}^v(t) = [\dot{x}(t), \dot{y}(t)]$ respectively. $\boldsymbol{f}$ is known as the drift function, $\boldsymbol{Q}$ is the diffusion matrix, $\boldsymbol{w}(t)$ denotes the n-dimensional standard Brownian notion which is independent of $\boldsymbol{x}(t)$. The measurement $z_k \in \mathbb{R}^d$, $h : \mathbb{R}^n \times R \to \mathbb{R}^d$, the measurement noise $e_k \in \mathbb{R}^n$ is independent Gaussian with zero mean and known covariance matrix $\boldsymbol{R}$.

III. CONTINUOUS-DISCRETE FILTERING

The one of the main differences between discrete-discrete and continuous-discrete filtering methods is concentrated in the state prediction. The interval within adjacent measurements is divided in several small intervals; the state is predicted at each small interval. In general, Euler approximation, Taylor approximation and Runge-Kutta approximation are used widely for the state propagation in the CD filtering methods. Though the forms of those two approximation methods are quite different, the core is to realize state propagation in the small intervals. Here, The Itô-Taylor of 1.5 order based CD-CKF is introduced. The details of CD-CKF algorithm can be referred to [7].

For the interval $(t, t+\delta)$, the state

$$\begin{aligned}\boldsymbol{x}(t+\delta) &= \boldsymbol{x}(t) + \delta \boldsymbol{f}(\boldsymbol{x}(t), t) \\ &\quad + \frac{1}{2}\delta^2(\Gamma_0 \boldsymbol{f}(\boldsymbol{x}(t), t) + \sqrt{\boldsymbol{Q}}\boldsymbol{\beta} + (\Gamma \boldsymbol{f}(\boldsymbol{x}(t), t))\boldsymbol{\gamma}\end{aligned} \tag{4}$$

where δ is a small interval, $\boldsymbol{\beta}$ is a Gaussian random variable related to the standard Gaussian random $\boldsymbol{u}$ via $\boldsymbol{\beta} = \sqrt{\delta}\boldsymbol{u} \sim N(0, \delta \boldsymbol{I}_n)$. Two differential operators Γ_0 and Γ are defined by

$$\begin{aligned}\Gamma_0 &= \frac{\partial}{\partial t} + \sum_{i=1}^{n} \boldsymbol{f}_i \frac{\partial}{\partial \boldsymbol{x}_i} \\ &\quad + \frac{1}{2}\sum_{j,p,q=1}^{n} \sqrt{\boldsymbol{Q}}_{p,j}\sqrt{\boldsymbol{Q}}_{q,j}\frac{\partial^2}{\partial \boldsymbol{x}_p \partial \boldsymbol{x}_q} \\ \Gamma_j &= \sum_{i=1}^{n} \sqrt{\boldsymbol{Q}}_{i,j}\frac{\partial}{\partial \boldsymbol{x}_i}\end{aligned}$$

The term $\Gamma \boldsymbol{f}(\cdot)$ represents a square matrix with its (i, j) th element being $\Gamma_i \boldsymbol{f}_j(\cdot)$, $i, j = 1, \ldots, n$.

Suppose the interval within adjacent measurements is divided in m small intervals δ, $\delta = T/m$, t is the measurement period. The interval $g \in (1, m)$, when $g = 1$, the state estimate

$$\begin{aligned}\hat{\boldsymbol{x}}_{k|k}^1 &= \mathrm{E}[\boldsymbol{x}_k^1 \,|z_{1:k}] \\ &\approx \mathrm{E}[\boldsymbol{f}_d(\boldsymbol{x}_k, kT) + \sqrt{\boldsymbol{Q}}\boldsymbol{\beta} + \Gamma \boldsymbol{f}(\boldsymbol{x}_k, kT)\boldsymbol{\gamma} \,|z_{1:k}]\end{aligned} \tag{5}$$

Because the noise terms are independent of the state vector and zero-mean Guassian, we may further simplify matters by writting

$$\begin{aligned}\hat{\boldsymbol{x}}_{k|k}^1 &= \mathrm{E}[\boldsymbol{x}_k^1 \,|z_{1:k}] \\ &= \int \boldsymbol{f}_d(\boldsymbol{x}_k, kT)N(\boldsymbol{x}_k; \hat{\boldsymbol{x}}_{k|k}, \boldsymbol{P}_{k|k})d\boldsymbol{x}_k\end{aligned} \tag{6}$$

where $N(\boldsymbol{x}_k; \hat{\boldsymbol{x}}_{k|k}, \boldsymbol{P}_{k|k})$ is the statistic of $\boldsymbol{x}_k$.

For CD-CKF, the state predicted error covariance matrix is also propagated as

$$\begin{aligned}\boldsymbol{P}_{k|k}^{1} \approx & \int_{\mathbb{R}^n} \boldsymbol{f}_d(\boldsymbol{x}_k, kT)\boldsymbol{f}_d^T(\boldsymbol{x}_k, kT)N(\boldsymbol{x}_k; \hat{\boldsymbol{x}}_{k|k}, \boldsymbol{P}_{k|k})d\boldsymbol{x}_k \\ & + \frac{\delta^3}{3}(\Gamma \boldsymbol{f}(\hat{\boldsymbol{x}}_{k|k}, kT)(\Gamma \boldsymbol{f}(\hat{\boldsymbol{x}}_{k|k}, kT)^T \\ & + \frac{\delta^2}{2}[\sqrt{\boldsymbol{Q}}(\Gamma \boldsymbol{f}(\hat{\boldsymbol{x}}_{k|k}, kT)^T + (\Gamma \boldsymbol{f}(\hat{\boldsymbol{x}}_{k|k}, kT)\sqrt{\boldsymbol{Q}}^T] \\ & - (\hat{\boldsymbol{x}}_{k|k}^1)(\hat{\boldsymbol{x}}_{k|k}^1)^T + \delta \boldsymbol{Q} \end{aligned} \tag{7}$$

Based on the third-degree cubature rule, we have

$$\hat{\boldsymbol{x}}_{k|k}^1 \approx \frac{1}{2n}\sum_{i=1}^{2n} \boldsymbol{X}_{i,k|k}^{*(1)} \tag{8}$$

where

$$\boldsymbol{X}_{i,k|k}^{*(1)} = f_d(\hat{\boldsymbol{x}}_{k|k} + \sqrt{\boldsymbol{P}_{k|k}}\xi_i, kT) \tag{9}$$

Thus the predicted error covariance matrix can be written as

$$\begin{aligned}\boldsymbol{P}_{k|k}^{1} \approx & (\Delta \boldsymbol{X}_{k|k}^{*(1)})(\Delta \boldsymbol{X}_{k|k}^{*(1)})^T \\ & + \frac{\delta^3}{3}(\Gamma \boldsymbol{f}(\hat{\boldsymbol{x}}_{k|k}, kT)(\Gamma \boldsymbol{f}(\hat{\boldsymbol{x}}_{k|k}, kT)^T \\ & + \frac{\delta^2}{2}[(\Gamma \boldsymbol{f}(\hat{\boldsymbol{x}}_{k|k}, kT)\boldsymbol{Q}^T + \boldsymbol{Q}(\Gamma \boldsymbol{f}(\hat{\boldsymbol{x}}_{k|k}, kT)^T] + \delta \boldsymbol{Q}\end{aligned} \tag{10}$$

where

$$\Delta \boldsymbol{X}_{k|k}^{*(1)} = \frac{1}{\sqrt{2n}}\left[\Delta \boldsymbol{X}_{1,k|k}^{*(1)} - \hat{\boldsymbol{x}}_{k|k}^1, \cdots, \Delta \boldsymbol{X}_{2n,k|k}^{*(1)} - \hat{\boldsymbol{x}}_{k|k}^1\right] \tag{11}$$

IV. THE ADAPTIVE FEEDBACK FRAMEWORK

Above section illustrated the basic CD-CKF method. Considering the unpredicted error in the state prediction, the adaptive stochastic feedback CD-CKF is proposed in this section, in which the covariance is estimated by the maximum likelihood estimation method. In this section, the covariance estimation based on the maximum likelihood estimation is introduced, and then the whole framework will be illustrated.

A. COVARIANCE ADAPTION

In CD-CKF, the updated state is

$$\hat{\boldsymbol{x}}_{k+1|k+1} = \hat{\boldsymbol{x}}_{k+1|k} + \boldsymbol{W}_{k+1}\boldsymbol{e}_{k+1} \tag{12}$$

where the continuous-discrete cubature gain is

$$\boldsymbol{W}_{k+1} = \boldsymbol{P}_{xz,k+1|k}\boldsymbol{P}_{zz,k+1|k}^{-1} \tag{13}$$

$\boldsymbol{P}_{xz,k+1|k}$ and $\boldsymbol{P}_{zz,k+1|k}$ are cross-covariance matrix and innovations covariance matrix respectively.

The error covariance matrix is

$$\boldsymbol{P}_{k+1|k+1} = \boldsymbol{P}_{k+1|k} - \boldsymbol{W}_{k+1}\boldsymbol{P}_{zz,k+1|k}\boldsymbol{W}_{k=1}^T \tag{14}$$

The innovation

$$\boldsymbol{e}_{k+1} = z_{k+1} - \hat{z}_{k+1|k} \tag{15}$$

where the predicted measurement

$$\hat{z}_{k+1|k} = \frac{1}{2n}\sum_{i=1}^{2n} h(\boldsymbol{X}_{i,k+1|k}, k+1) \approx \boldsymbol{H}\hat{\boldsymbol{x}}_{k+1|k} \tag{16}$$

where $x_{i,k+1|k}$ is the cubature points, $\boldsymbol{H}$ is the Jacobian matrix of partial derivatives of h.

The innovations covariance matrix is

$$\boldsymbol{P}_{zz,k+1|k} = \boldsymbol{Z}_{k+1|k}\boldsymbol{Z}_{k+1|k}^T + \boldsymbol{R}_{k+1} \tag{17}$$

where the weighted-centered matrix is

$$\boldsymbol{Z}_{k+1|k} = \frac{1}{\sqrt{2n}}\left[z_{1,k+1|k} - \hat{z}_{k+1|k}, \cdots, z_{2n,k+1|k} - \hat{z}_{k+1|k}\right] \tag{18}$$

Substituting (15) and (16) to (17), the innovations covariance matrix can be described as

$$\boldsymbol{P}_{zz,k+1|k} \approx \boldsymbol{H}\boldsymbol{P}_{k+1|k}\boldsymbol{H}^T + \boldsymbol{R}_{k+1} \tag{19}$$

where $\boldsymbol{P}_{k+1|k}$ is $\boldsymbol{P}_{k|k}^g$ when $g \to m$.

The cross-covariance matrix

$$\begin{aligned}&\boldsymbol{P}_{xz,k+1|k} \\ &= \boldsymbol{X}_{k+1|k}\boldsymbol{Z}_{k+1|k}^T \\ &= \frac{1}{\sqrt{2n}}\left[\Delta \boldsymbol{X}_{1,k|k}^{*(k+1)} - \hat{\boldsymbol{x}}_{k|k}^{(k+1)}, \cdots, \Delta \boldsymbol{X}_{2n,k|k}^{*(k+1)} - \hat{\boldsymbol{x}}_{k|k}^{(k+1)}\right] \\ &\quad \cdot \frac{1}{\sqrt{2n}}\left[z_{1,k+1|k} - \hat{z}_{k+1|k}, \cdots, z_{2n,k+1|k} - \hat{z}_{k+1|k}\right]^T\end{aligned} \tag{20}$$

Substituting (17) to (20), we can get

$$\boldsymbol{P}_{xz,k+1|k} \approx \boldsymbol{P}_{k|k}^j\boldsymbol{H}^T, \quad j = k+1 \tag{21}$$

Namely, $\boldsymbol{P}_{xz,k+1|k} \approx \boldsymbol{P}_{k+1|k}\boldsymbol{H}^T$. Then, the continuous-discrete cubature gain can be written as

$$\boldsymbol{W}_{k+1} \approx \boldsymbol{P}_{k+1|k}\boldsymbol{H}^T\boldsymbol{P}_{zz,k+1|k}^{-1} \tag{22}$$

In order to decrease the unpredicted error, the prior error covariance is considered to be reconstructed. Suppose that the covariance $\boldsymbol{P}_{j+1|i}, j = k-N+1, \ldots, k+1$ is nearly constant. This assumption is a simplification used in [18] and [19], and is proved to be an explicit and efficient method applied for online estimation.

The maximum likelihood estimation problem can be described as

$$\begin{aligned}L(\boldsymbol{P}_{k+1|k}) &= \ln p(\boldsymbol{e}_{k-N+1}, \cdots, \boldsymbol{e}_k \left|\boldsymbol{P}_{k+1|k}\right.) \\ &= \sum_{j=k-N+1}^{k} \ln p(\boldsymbol{e}_j \left|\boldsymbol{P}_{k+1|k}\right.)\end{aligned} \tag{23}$$

where n is the time window, $\boldsymbol{e}_j$ can be regarded as a normally distributed random variable. The portability $p(\cdot)$ can be written as

$$p(\boldsymbol{e}_j \left|\boldsymbol{P}_{k+1|k}\right.) = \frac{1}{\sqrt{(2\pi)^m \left|\boldsymbol{P}_{zz,j+1|j}\right|}} \exp\left(-\frac{1}{2}\boldsymbol{e}_j^T\boldsymbol{P}_{zz,j+1|j}\boldsymbol{e}_j\right) \tag{24}$$

$L(\boldsymbol{P}_{k+1|k})$ is a scalar and $\boldsymbol{P}_{k+1|k}$ is a symmetric with size $n \times n$. For derivative $\Omega_{k+1} = \partial L(\boldsymbol{P}_{k+1|k})/\partial \boldsymbol{P}_{k+1|k}$, the s-th row and t-th column element of the derivative is

$$\Omega_{k+1}^{s,t} = -\frac{1}{2}\mathrm{tr}\left\{\sum_{j=k-N+1}^{k}[\Theta \cdot \Psi]\right\} \tag{25}$$

$$\Theta = \boldsymbol{P}_{zz,j+1|j}^{-1} - \boldsymbol{P}_{zz,j+1|j}^{-1}\boldsymbol{e}_j\boldsymbol{e}_j^T\boldsymbol{P}_{zz,j+1|j}^{-1} \tag{26}$$

$$\Psi = \frac{\partial \boldsymbol{P}_{zz,j+1|j}}{\partial \boldsymbol{P}_{k+1|k}^{s,t}} \tag{27}$$

where $\boldsymbol{P}_{k+1|k}^{s,t}$ is the s-th row and t-th column element of $\boldsymbol{P}_{k+1|k}$. Then $\hat{\boldsymbol{P}}_{k+1|k}$ can be yielded by setting Ω_{k+1} to zero, i.e. $\Omega_{k+1}^{s,t} = 0$.

Because $\boldsymbol{R}_{k+1}$ and $\boldsymbol{H}$ are independent of $\boldsymbol{P}_{k+1|k}$, with (19) and (27), we can get

$$\Psi = \boldsymbol{H}\frac{\partial \boldsymbol{P}_{k+1|k}}{\partial \boldsymbol{P}_{k+1|k}^{s,t}}\boldsymbol{H}^T \tag{28}$$

$$tr\left\{\sum_{j=k-N+1}^{k}\left[\Theta \cdot \boldsymbol{H}\frac{\partial \boldsymbol{P}_{k+1|k}}{\partial P_{k+1|k}^{s,t}}\boldsymbol{H}^T\right]\right\} = 0 \tag{29}$$

Then pre- and post-multiply the matrix inside $tr\{\cdot\}$ by $\boldsymbol{H}^T$ and its inverse (or the generalized inverse) can be expressed as

$$tr\left\{\sum_{j=k-N+1}^{k}\left[\boldsymbol{H}^T\Theta \cdot \boldsymbol{H}\frac{\partial \boldsymbol{P}_{k+1|k}}{\partial \boldsymbol{P}_{k+1|k}^{s,t}}\right]\right\} = 0 \tag{30}$$

because $\frac{\partial \boldsymbol{P}_{k+1|k}}{\partial \boldsymbol{P}_{k+1|k}^{s,t}}$ is a constant matrix and its s-th row and t-th column element is 1 while other elements are 0. Based on the multiplication rule, the t-th column of the matrix $\boldsymbol{H}^T\Theta\boldsymbol{H} \cdot \frac{\partial \boldsymbol{P}_{k+1|k}}{\partial \boldsymbol{P}_{k+1|k}^{s,t}}$ cannot be 0 while other column must be 0. So the value of $tr\{\cdot\}$ is equal to the t-th diagonal element of $\{\cdot\}$,

$$\left\{\sum_{j=k-N+1}^{k}\left[\boldsymbol{H}^T\Theta \cdot \boldsymbol{H}\frac{\partial \boldsymbol{P}_{k+1|k}}{\partial \boldsymbol{P}_{k+1|k}^{s,t}}\right]\right\}^{t,t} = 0 \tag{31}$$

Furthermore, because the s-th row and t-th column element of $\frac{\partial \boldsymbol{P}_{k+1|k}}{\partial \boldsymbol{P}_{k+1|k}^{s,t}}$ is 1 and other elements are 0, to insure elements of $\{\cdot\}$ to be 0, we can obtain

$$\sum_{j=k-N+1}^{k}\left\{\left[\boldsymbol{H}^T\Theta \cdot \boldsymbol{H}\right]\right\}^{t,s} = 0 \tag{32}$$

where t, s can be any value within (0,n), so

$$\sum_{j=k-N+1}^{k}\left[\boldsymbol{H}^T\Theta \cdot \boldsymbol{H}\right] = 0 \tag{33}$$

Let's multiply both sides of (33) by $\boldsymbol{P}_{j+1|j}$,

$$\sum_{j=k-N+1}^{k}\left[\boldsymbol{P}_{j+1|j}\boldsymbol{H}^T\Theta \cdot \boldsymbol{H}\boldsymbol{P}_{j+1|j}\right] = 0 \tag{34}$$

With (22) and (26),

$$\sum_{j=k-N+1}^{k}\left[\boldsymbol{W}_{j+1}\boldsymbol{H}\boldsymbol{P}_{j+1|j} - \boldsymbol{W}_{j+1}\boldsymbol{e}_j\boldsymbol{e}_j^T\boldsymbol{W}_{j+1}^T\right] = 0 \tag{35}$$

Based on (12) and (14), we can obtain

$$\boldsymbol{W}_{j+1}\boldsymbol{e}_j = \Delta\hat{\boldsymbol{x}}_{j+1} = \hat{\boldsymbol{x}}_{j+1|j+1} - \hat{\boldsymbol{x}}_{j+1|j} \tag{36}$$

$$\sum_{j=k-N+1}^{k}\left[\boldsymbol{P}_{j+1|j} - \boldsymbol{P}_{j+1|j+1} - \Delta\hat{\boldsymbol{x}}_{j+1}\Delta\hat{\boldsymbol{x}}_{j+1}^T\right] = 0 \tag{37}$$

Then

$$\sum_{j=k-N+1}^{k}\boldsymbol{P}_{j+1|j} = \sum_{j=k-N+1}^{k}\left(\boldsymbol{P}_{j+1|j+1} + \Delta\hat{\boldsymbol{x}}_{j+1}\Delta\hat{\boldsymbol{x}}_{j+1}^T\right) \tag{38}$$

Considering the assumption, $\boldsymbol{P}_{k+1|k}$ can be approximated by

$$\hat{\boldsymbol{P}}_{k+1|k} = \frac{1}{n}\sum_{j=k-N+1}^{k}\boldsymbol{P}_{j+1|j} = \sum_{j=k-N+1}^{k}\boldsymbol{P}_{j+1}^{*} \tag{39}$$

where $\boldsymbol{P}_{j+1}^{*}$ is defined as an intermediate matrix. Hence,

$$\hat{\boldsymbol{P}}_{k+1|k} = \hat{\boldsymbol{P}}_{k|k-1} + \left(\boldsymbol{P}_k^{*} - \boldsymbol{P}_{k-N}^{*}\right) \tag{40}$$

B. THE DISCRIMINANT RULE

The covariance adaption method is demonstrated in the above section. The key is to decide when to use the adaption method. Let's reconsider the assumption that the covariance $\boldsymbol{P}_{j+1|j}, j = k-N+1, \ldots, k+1$ is nearly constant. Actually, a discriminant rule is needed to judge whether the covariance is nearly constant or not. In order to measure the difference between two covariance matrices at adjacent times, similarity measurement method is used, which is applied widely for machine learning.

From the viewpoint of matrix, each element should be compared with the corresponding one of the covariance at adjacent time, if the difference was small, the covariance matrices at adjacent times can be considered to be constant. Chebyshev distance of these two covariance matrices is used.

Chebyshev distance is defined as

$$\lim_{p\to\infty}\left(\sum_{s,t=1}^{n}\left|\boldsymbol{P}_{j+1|j}^{s,t} - \boldsymbol{P}_{j|j-1}^{s,t}\right|^p\right)^{\frac{1}{p}} = \max_{s,t=1}^{n}\left|\boldsymbol{P}_{j+1|j}^{s,t} - \boldsymbol{P}_{j|j-1}^{s,t}\right| \tag{41}$$

where $\boldsymbol{P}_{j+1|j}^{s,t}$ is the the s-th row and t-th column element of $\boldsymbol{P}_{j+1|j}$.

Normally, the diagonal elements of the covariance matrix are larger than other elements, thus the covariance matrix is diagonally dominant when the filtering tends to be stable. The maximum differences of elements defined by Chebyshev distance are from the diagonal elements. The diagonal elements represent the variance of the state, so the differences of corresponding diagonal elements are the differences of the states' error variance at adjacent time. Thus the threshold of

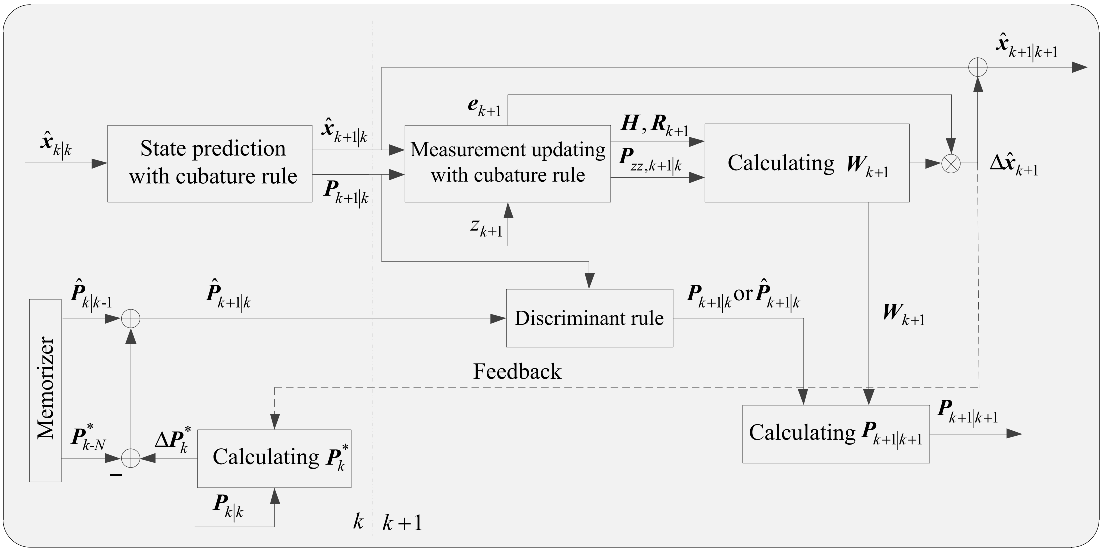

FIGURE 1. Adaptive feedback framework.

the discriminant rule is defined by Geometrical Dilution of Precision (GDOP)

$$\max_{s,t=1}^{n} \left| P^{s,t}_{j+1|j} - P^{s,t}_{j|j-1} \right| \le R_{k+1} \tag{42}$$

where R_{k+1} is the covariance of the measurement noise, which is generally constant.

C. ADAPTIVE FEEDBACK FRAMEWORK

According to the above theoretical analysis, the diagram of adaptive feedback framework is shown in Figure 1. At time k, the state $\hat{x}_{k|k}$ is predicted according to the cubature rule, and then $\hat{x}_{k+1|k}$ and $P_{k+1|k}$ are propagated. When the measurement z_{k+1} is input, the innovations covariance matrix $P_{zz,k+1|k}$ is calculated by the cubature rule, the Jacobian matrix H and the covariance of the measurement noise R_{k+1} are also generated to calculate the cubature gain W_{k+1}. In this process, the covariance matrice $P_{k+1|k}$ is tested according to the discriminant rule to determine whether the adaptive feedback can be triggered or not. If the covariance matrice $P_{k+1|k}$ meet the condition defined by (42), the adaptive feedback mechanism will be triggered, and $P_{k+1|k}$ will be replaced by $\hat{P}_{k+1|k}$ generated by (40). At last, the error covariance matrix is generated. The details of the algorithm are in the Appendix.

The characteristics of adaptive feedback framework can be concluded as:

Remark 1: the adaptive feedback channel separates the covariance estimation from the traditional filtering framework. It is the novel way proposed in this study to avoid the unpredictable errors.

Remark 2: the complex process of numerical integration or discretization in SDE is not needed in the covariance propagation, the computational efficiency is improved.

Remark 3: CD-CKF in the framework enables the ASFCD-CKF to deal with the nonlinear filtering problem better.

V. NUMERICAL SIMULATION

In this section, a linear model and a nonlinear model are used to investigate the filtering performance of ASFCD-CKF. Herein, CD-EKF [20], 1.5 order CD-CKF [7], SFCD-EKF [17] (which is also called CD-AKF) and SFCD-CKF (stochastic feedback CD-CKF) are compared. Specially, "linear" and "non-linear" described here refer to the type of state models, because the measurement models in BOT are all non-linear in this study. The simulations are conducted in Matlab 7.0 using Windows XP, Intel Core i3, 3.3 GHz platform. Monte Carlo simulations are set to be 200 times for each scenario.

A. LINEAR MODEL

The linear state model is

$$\mathrm{d}x(t) = Fx(t)\mathrm{d}t + \sqrt{Q}\mathrm{d}v(t) \tag{43}$$

where $v(t)$ is the standard Brownian notion, F is the state transition matrix. Measurement function is (2). The measurement noise is $e_k \sim N(0, 10^{-2})$. The time window $N = 5$, the measurement sampling interval $T = 1$ min. The motion of observer is the CA model with the constant acceleration is $[0.1m/s^2, 0m/s^2]^T$. The initial state of observer is $\left[0m, 0m, 100m/s, 50m/s\right]^T$. The initial state of Target is $\left[1\times10^5m, 1\times10^5m, 40m/s, -190m/s\right]^T$. The diffusion matrix is

$$Q = \begin{bmatrix} T^3/3 & 0 & T^2/2 & 0 \\ 0 & T^3/3 & 0 & T^2/2 \\ T^2/2 & 0 & T & 0 \\ 0 & T^2/2 & 0 & T \end{bmatrix} \cdot 10^{-5}$$

$$F = \begin{bmatrix} 1 & 0 & T & 0 \\ 0 & 1 & 0 & T \\ 0 & 0 & 1 & 0 \\ 0 & 0 & 0 & 1 \end{bmatrix}$$

The root mean square error (RMSE) of position is applied to evaluate the accuracy of BOT.

$$\mathrm{RMSE}(k) = \left(\frac{1}{N_{\mathrm{MC}}} \sum_{i=1}^{N_{\mathrm{MC}}} \left\| \boldsymbol{x}_k - \hat{\boldsymbol{x}}_k^i \right\|_2^2 \right)^{1/2} \tag{44}$$

where N_{MC} is the number of Monte Carlo simulations, $\hat{\boldsymbol{x}}_k^i$ is the estimation at time k for Monte Carlo simulation i, $\boldsymbol{x}_k$ is the real state of the target.

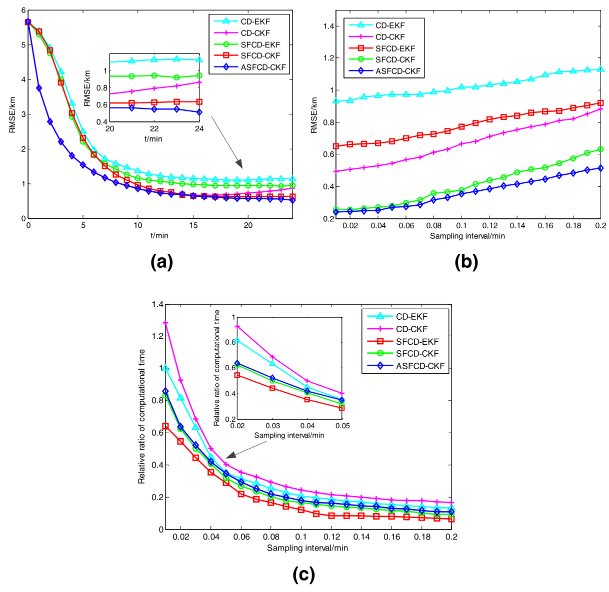

FIGURE 2. Performances comparison with the linear model. (a) The RMSEs comparison. (b) The RMSEs with different sampling intervals. (c) The relative ratio of the computational time.

Figure 2 presents the comparison results of filtering performances. Figure 2 (a) shows the RMSE with different filtering methods. The RMSEs of CD-CKF and ASFCD-CKF are the same in the first 13s, because adaptive stochastic feedback is not used in this stage, and then the working condition of the feedback has not met the requirements of the discriminant rule. After this initial stage, the RMSE of ASFCD-CKF is the lowest and the final value is 19.05% lower than CD-CKF. The performances of CD-CKF and SFCD-EKF are superior over CD-EKF. Figure 2 (b) shows the RMSE with different sampling intervals. In general, the RMSE will be decrease along with the decrease of sampling interval. The RMSEs of CD-CKF and ASFCD-CKF are similar when the sampling interval approaches to 0.01min. Figure 2(c) shows the relative ratio of the computational time, CD-EKF with sampling interval 0.01 is the datum point. SFCD-EKF exhibits the highest computational efficiency, while CD-CKF is contrary, ASFCD-CKF and SFCD-CKF are not better than SFCD-EKF. The reasons are: firstly, stochastic framework avoids the complex computation in the filtering methods, and thus can significantly improve the computational efficiency. Secondly, the computational complexity of CD-CKF is higher than CD-EKF. As a result, SFCD-EKF is superior over other methods; SFCD-CKF and ASFCD-CKF are better than CD-CKF and CD-EKF but lower than SFCD-EKF. On the whole, ASFCD-CKF has the advantage on estimation accuracy and computational efficiency for filtering problem of linear model.

B. NONLINEAR MODEL

In this section, the nonlinear model [21] is defined as

$$\begin{cases} d\begin{bmatrix} y(t) \\ \dot{y}(t) \end{bmatrix} = \begin{bmatrix} \dot{y}(t) \\ \lambda(1 - x^2(t))\dot{y}(t) - x(t) \end{bmatrix} dt + \begin{bmatrix} 0 \\ 1 \end{bmatrix} dw(t) \\ \boldsymbol{x}(t) = \boldsymbol{x}(0) + \begin{bmatrix} t \\ y(t) \end{bmatrix} \end{cases} \tag{45}$$

The parameters $\lambda = 0.3$ and $w(t) \sim N(0, 10^{-5})$. The initial position is $\boldsymbol{x}(0) = \left[1 \times 10^5 m, 1 \times 10^5 m\right]^T$. The motion of observer is the same as the previous section. The measurement is defined by formula (2).

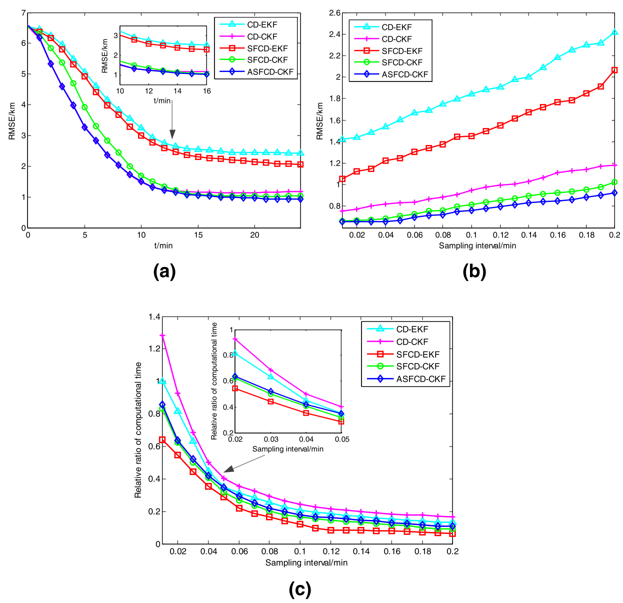

FIGURE 3. Performances comparison with the nonlinear model. (a) The RMSEs comparison. (b) The RMSEs with different sampling intervals. (c) The relative ratio of the computational time.

As shown in Figure 3 (a), the RMSE of CD-EKF is the highest, and it is similar to SFCD-EKF. The RMSE of SFCD-CKF is higher than CD-CKF and ASFCD-CKF in the first 13 minutes, and the RMSE of CD-CKF are the same as ASFCD-CKF. In this stage, the adaptive stochastic feedback is not triggered, only the framework of CD-CKF works. After this stage, the finial RMSE of ASFCD-CKF is 9.70% higher than SFCD-CKF and 20.64% higher than CD-CKF. Figure 3 (b) shows the RMSEs with different sampling intervals, the general tendency is: it is a positive correlation between the sampling intervals and the values of RMSEs. Figure 3 (c) shows the comparison of the computational time with different filtering methods. CD-EKF with sampling interval 0.01 is the datum point. With the increase of the sampling intervals, the computational time decreases. The computational efficiency of SFCD-EKF is superior over the other methods, and ASFCD-CKF and SFCD-CKF are a little higher. From the comprehensive perspective, ASFCD-CKF has the advantage in accuracy and computational efficiency. Although the computation efficiency is not the most superior, the adaptive stochastic feedback framework decreases the complex computation of framework of CD-CKF.

VI. CONCLUSION

The ASFCD-CKF method is proposed to alleviate effects of unpredictable errors. Different from the general framework of traditional filtering methods, the adaptive stochastic feedback channel is established to modify the framework of CD-CKF, in which the posterior covariance information is used to achieve the prior covariance. Chebyshev distance is applied to judge the proper condition for start-up of the feedback. The feedback channel divides the covariance updating from the complex mathematical calculation, and avoids the unpredictable errors, thus the performances of efficiency and accuracy are improved significantly. The numerical results illustrate the superior performances of the proposed method. However, the feedback channel will be violated by the significantly change of covariance. We will focus on this problem and extend the application scope of this method.

APPENDIX

Appendixes, if needed, appear before the acknowledgment.

Adaptive stochastic feedback continuous-discrete cubature Kalman filter (ASFCD-CKF)

Algorithm 1 Adaptive Stochastic Feedback Continuous-Discrete Cubature Kalman Filtering Algorithm

Initialization $g \to 0$, $\hat{\boldsymbol{x}}^0_{k|k} = \hat{\boldsymbol{x}}_{k|k}$ and $\boldsymbol{P}^0_{k|k} = \boldsymbol{P}_{k|k}$.

***m*-step Time-Update**

(1) Factorize

$$\boldsymbol{P}^g_{k|k} = (S^g_{k|k})(S^g_{k|k})^T$$

(2) Cubature points ($i = 1, 2, \ldots, 2n$)

$$\xi_i = \begin{cases} \sqrt{n}e_i, & i = 1, 2, \cdots, n \\ -\sqrt{n}e_i, & i = n+1, n+2, \cdots, 2n \end{cases}$$

$$\boldsymbol{x}^g_{i,k|k} = S^g_{k|k}\xi_i + \hat{\boldsymbol{x}}^g_{k|k}$$

(3) The propagated cubature point set

$$\boldsymbol{x}^{*(g+1)}_{i,k|k} = \boldsymbol{f}_d(\boldsymbol{x}^g_{i,k|k}, kT + g\delta)$$

(4) Estimate the predicted state

$$\boldsymbol{x}^{g+1}_{i,k|k} = \frac{1}{2n}\sum_{i=1}^{2n}\boldsymbol{x}^{*(g+1)}_{i,k|k}$$

Algorithm 1 *Continued.* Adaptive Stochastic Feedback Continuous-Discrete Cubature Kalman Filtering Algorithm

(5) Estimate the predicted error covariance matrix

$$\Delta\boldsymbol{X}^{*(g+1)}_{k|k} = \frac{1}{\sqrt{2n}}\left[\boldsymbol{x}^{*(g+1)}_{1,k|k} - \hat{\boldsymbol{x}}^{g+1}_{k|k}, \cdots, \boldsymbol{x}^{*(g+1)}_{2n,k|k} - \hat{\boldsymbol{x}}^{g+1}_{k|k}\right]$$

$$\begin{aligned}\boldsymbol{P}^{g+1}_{k|k} &= (\Delta\boldsymbol{X}^{*(g+1)}_{k|k})(\Delta\boldsymbol{X}^{*(g+1)}_{k|k})^T \\ &+ \frac{\delta^3}{3}(\Gamma\boldsymbol{f}(\hat{\boldsymbol{x}}^g_{k|k}, kT + g\delta)(\Gamma\boldsymbol{f}(\hat{\boldsymbol{x}}^g_{k|k}, kT + g\delta)^T \\ &+ \frac{\delta^2}{2}[(\Gamma\boldsymbol{f}(\hat{\boldsymbol{x}}^g_{k|k}, kT + g\delta)\boldsymbol{Q}^T \\ &+ \boldsymbol{Q}(\Gamma\boldsymbol{f}(\hat{\boldsymbol{x}}^g_{k|k}, kT + g\delta)^T] + \delta\boldsymbol{Q}\end{aligned}$$

Increase g by one and repeat the steps (1)-(5) until $g = m$-1. When $g \to m$,

(6) The standardized residual

$$\tau_{k+1} = \left(z_{k+1} - \hat{z}_{k+1|k}\right)/S_{zz,k+1|k}$$

(7) The innovation covariance

$$P_{zz,k+1|k} = S_{zz,k+1|k}S^T_{zz,k+1|k}$$

(8) The threshold

$$\begin{aligned}\lambda_{k+1} &= \left(z_{k+1} - \hat{z}_{k+1|k}\right)P^{-1}_{zz,k+1|k}\left(z_{k+1} - \hat{z}_{k+1|k}\right) \\ &= \tau^2_{k+1}\end{aligned}$$

(9) The discriminant rule

If $\max_{s,t=1}^{n}\left|\boldsymbol{P}^{s,t}_{j+1|j} - \boldsymbol{P}^{s,t}_{j|j-1}\right| \geq \boldsymbol{R}_{k+1}$

$$\boldsymbol{P}_{k+1|k} = \boldsymbol{P}^m_{k|k}$$

else

$$\hat{\boldsymbol{P}}_{k+1|k} = \frac{1}{N}\sum_{j=k-N+1}^{k}\boldsymbol{P}_{j+1|j}$$

end

Measurement-Update

(1) Factorize

$$\boldsymbol{P}_{k+1|k} = S_{k+1|k}S^T_{k+1|k}$$

(2) Evaluate the cubature points ($i = 1, \ldots, 2n$)

$$\boldsymbol{X}_{i,k+1|k} = S_{k+1|k}\xi_i + \hat{\boldsymbol{x}}_{k+1|k}$$

(3) Evaluate the propagated cubature points

$$z_{i,k+1|k} = h(\boldsymbol{X}_{i,k+1|k}, k+1)$$

(4) Estimate the predicted measurement

$$\hat{z}_{k+1|k} = \frac{1}{2n}\sum_{i=1}^{2n} z_{i,k+1|k}$$

Algorithm 1 *Continued.* Adaptive Stochastic Feedback Continuous-Discrete Cubature Kalman Filtering Algorithm

(5) Estimate the innovations covariance matrix

$$\boldsymbol{P}_{zz,k+1|k} = z_{k+1|k} z_{k+1|k}^{T} + \sigma^2$$

where the weighted-centered matrix

$$z_{k+1|k} = \frac{1}{\sqrt{2n}} \left[z_{1,k+1|k} - \hat{z}_{k+1|k}, \cdots, z_{2n,k+1|k} - \hat{z}_{k+1|k} \right]$$

(6) Estimate the cross-covariance matrix

$$\boldsymbol{P}_{xz,k+1|k} = \boldsymbol{X}_{k+1|k} z_{k+1|k}^{T}$$

where the weighted-centered matrix

$$\boldsymbol{X}_{k+1|k} = \frac{1}{\sqrt{2n}} \left[\boldsymbol{X}_{1,k+1|k} - \hat{\boldsymbol{x}}_{k+1|k}, \cdots, \boldsymbol{X}_{2n,k+1|k} - \hat{\boldsymbol{x}}_{k+1|k} \right]$$

(7) Estimate the continuous-discrete cubature gain

$$\boldsymbol{W}_{k+1} = \boldsymbol{P}_{xz,k+1|k} \boldsymbol{P}_{zz,k+1|k}^{-1}$$

(8) Estimate the updated state

$$\hat{\boldsymbol{x}}_{k+1|k+1} = \hat{\boldsymbol{x}}_{k+1|k} + \boldsymbol{W}_{k+1}(z_{k+1|k} - \hat{z}_{k+1|k})$$

(9) Estimate the corresponding error covariance matrix

$$\boldsymbol{P}_{k+1|k+1} = \boldsymbol{P}_{k+1|k} - \boldsymbol{W}_{k+1} \boldsymbol{P}_{zz,k+1|k} \boldsymbol{W}_{k+1}^{T}$$

CONFLICTS OF INTEREST

The authors declare no conflict of interest.

REFERENCES

[1] H. Zhang, B. de Saporta, F. Dufour, D. Laneuville, and A. Nègre, "Stochastic control of observer trajectory in passive tracking with acoustic signal propagation optimisation," *IET Radar, Sonar Navigat.*, vol. 12, no. 1, pp. 112–120, 2018.

[2] H. Zhang, B. de Saporta, and F. Dufour, "Quantization and stochastic control of trajectories of under water vehicle in bearings-only tracking," *IET Radar Sonar Navigat.*, vol. 12, no. 1, pp. 112–120, 2017.

[3] R. Radhakrishnan, S. Bhaumik, and N. K. Tomar, "Continuous-discrete shifted Rayleigh filter for underwater passive bearings-only target tracking," in *Proc. 11th Asian Control Conf.*, Gold Coast, QLD, Australia, Dec. 2017, pp. 795–800.

[4] D. Crouse, "Basic tracking using nonlinear continuous-time dynamic models," *IEEE Aerosp. Electron. Syst. Mag.*, vol. 30, no. 2, pp. 4–41, Feb. 2015.

[5] P. E. Kloeden and E. Okateb, *Numerical Solution of Stochastic Differential Equations*. Berlin, Germany: Springer, 1999.

[6] M. Murata and K. Hiramatsu, "Non-Gaussian filters for nonlinear continuous–discrete models," *SICE J. Control*, vol. 10, no. 2, pp. 53–61, 2017.

[7] I. Arasaratnam, S. Haykin, and T. R. Hurd, "Cubature Kalman filtering for continuous–discrete systems: Theory and simulations," *IEEE Trans. Signal Process.*, vol. 58, no. 10, pp. 4977–4993, Oct. 2010.

[8] D. F. Crouse, "Cubature Kalman filters for continuous-time dynamic models Part I: Solutions discretizing the Langevin equation," in *Proc. IEEE Radar Conf.*, Cincinnati, OH, USA, May 2014, pp. 0169–0174.

[9] G. Y. Kulikov and K. V. Maria, "Accurate continuous–discrete unscented Kalman filtering for estimation of nonlinear continous-time stochastic models in radar tracking," *Signal Process.*, vol. 139, pp. 25–35, Oct. 2017.

[10] D. F. Crouse, "Cubature Kalman filters for continuous-time dynamic models Part II: A solution based on moment matching," in *Proc. IEEE Radar Conf.*, Cincinnati, OH, USA, May 2014, pp. 0194–0199.

[11] S. Särkkä, J. Hartikainen, I. S. Mbalawata, and H. Haario, "Posterior inference on parameters of stochastic differential equations via non-linear Gaussian filtering and adaptive MCMC," *Statist. Comput.*, vol. 25, no. 2, pp. 427–437, 2015.

[12] T. Yang, H. A. P. Blom, and P. G. Mehta, "The continuous–discrete time feedback particle filter," in *Proc. Amer. Control Conf.*, Portland, OR, USA, 2014, pp. 648–653.

[13] K. V. Maria and G. Y. Kulikov, "On computational robustness of accurate continuous–discrete unscented Kalman filtering for target tracking models," in *Proc. Eur. Control Conf.*, Aalborg, Denmark, Jun./Jul. 2016, pp. 1129–1134.

[14] K. V. Maria and G. Y. Kulikov, "NIRK-based accurate continuous–discrete extended Kalman filters for estimating continuous-time stochastic target tracking models," *J. Comput. Appl. Math.*, vol. 316, pp. 260–270, May 2017.

[15] G. Y. Kulikov and M. V. Kulikova, "Accurate state estimation in continuous–discrete stochastic state-space systems with nonlinear or non-differentiable observations," *IEEE Trans. Autom. Control*, vol. 62, no. 8, pp. 4243–4250, Aug. 2017.

[16] T. Ogihara and H. Tanaka, "The euler method for continuous-time nonlinear filtering and stable convergence of conditional law," *Mathematics*, pp. 1–23, Oct. 2018.

[17] J. Wang, J. Wang, D. Zhang, and X. Shao, "Stochastic feedback based Kalman filter for nonlinear continuous–discrete systems," *IEEE Trans. Autom. Control*, vol. 63, no. 9, pp. 3002–3009, Sep. 2017.

[18] A. H. Mohamed and K. P. Schwarz, "Adaptive Kalman filtering for INS/GPS," *J. Geodesy*, vol. 73, no. 4, pp. 193–203, 1999.

[19] R. K. Mehra, "Approaches to adaptive filtering," *IEEE Trans. Autom. Control*, vol. AC-17, no. 5, pp. 693–698, Oct. 1972.

[20] M. Mallich, K. Morelande, and L. Mihaylova, "Continuous-discrete filtering using EKF, UKF, and PF," in *Proc. 15th Int. Conf. Inf. Fusion*, Singapore, 2012, pp. 1087–1094.

[21] G. Y. Kulikov and M. V. Kulikova, "Accurate numerical implementation of the continuous–discrete extended Kalman filter," *IEEE Trans. Autom. Control*, vol. 59, no. 1, pp. 273–279, Jan. 2014.

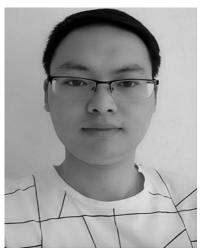

RENKE HE was born in 1993. He received the B.S. and M.S. degrees from the Air Force Engineering University, Xi'an, China, in 2014 and 2016, respectively, where he is pursuing the Ph.D. degree in control science and engineering. His current research interests include target tracking and signal processing.

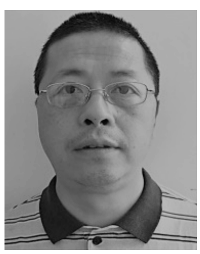

SHUXIN CHEN was born in 1965. He received the B.S. degree from the Department of Electronic Technology, National University of Defense Technology, Changsha, China, in 1987, the M.S. degree from the Department of Electronic Engineering, Xidian University, Xi'an, China, in 1993, and the Ph.D. degree from the Department of Electronic Engineering, Northwestern Polytechnical University, Xi'an, China, in 2002. He is currently a Professor with Air Force Engineering University. His research interests include signal processing and communication theory.

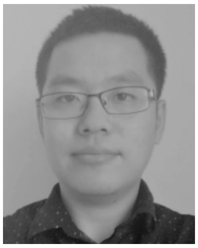

HAO WU was born in 1988. He received the M.S. and Ph.D. degrees from Air Force Engineering University, Xi'an, China, in 2012 and 2016, respectively, where he is currently a Lecturer. His research interests are signal processing and bearings-only tracking.

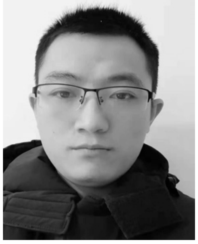

HAN XU was born in 1994. He is a Post-Graduate Student with Air Force Engineering University, Xi'an, China. His major is control science and engineering. His current research interests include target tracking and signal processing.

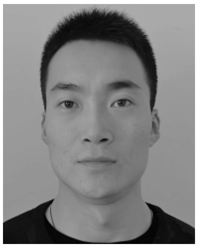

KUN CHEN was born in 1989. He received the M.S. and Ph.D. degrees from the Department of Navigation Engineering, Air Force Engineering University, Xi'an, China, in 2013 and 2017, respectively. His research interests include signal processing and navigation technology.

JING LIU was born in 1977. She received the M.S. degree from National University Defense Technology, Changsha, China, in 2011. She is currently a Lecturer with Air Force Engineering University. Her research interests are signal processing and communication theory.